Photon-Mediated Thermal Relaxation of Electrons in Nanostructures

D. R. Schmidt,[1] R. J. Schoelkopf,[2] and A. N. Cleland[1,*]

[1]*Department of Physics, University of California, Santa Barbara, California 93106, USA*

[2]*Department of Applied Physics and Physics, Yale University, New Haven, Connecticut 06520, USA*

(Received 28 August 2003; published 23 July 2004)

Measurements of the thermal properties of nanoscale electron systems have ignored the effect of electrical noise radiated between the electron gas and the environment, through the electrical leads. Here we calculate the effect of this photon-mediated process, and show that the low-temperature thermal conductance is equal to the quantum of thermal conductance, $G_Q = \pi^2 k_B^2 T/3h$, times a coupling coefficient. We find that, at very low temperatures, the photon conductance is the dominant route for thermal equilibration, while at moderate temperatures this relaxation mode adds one quantum of thermal conductance to that due to phonon transport.

DOI: 10.1103/PhysRevLett.93.045901 PACS numbers: 66.70.+f, 44.40.+a, 65.80.+n

A striking effect in one-dimensional systems is that the linear transport coefficients become quantized, in multiples of combinations of the fundamental constants: The specific material properties fade into the background. The observation of quantized charge conductance in quantum point contacts is the archetypal manifestation of this effect [1]. The concept of quantization has been extended to the thermal conductance of both electrons and phonons in confined geometries [2–9], with theoretical treatments verified by experiments. Here we discuss the impact of the related but quite distinct quantization of the *photon-mediated* thermal conductance, between an electron gas and its electromagnetic environment. The thermal conductance for photons yields a quantization condition quite similar to that for electrons and phonons, but due to the weakness of the electron-phonon coupling at low temperature this electromagnetic channel is the dominant thermal relaxation mode for an electron gas as $T \to 0$. Furthermore, in the limit where the electron gas can be treated as a single lumped electrical element, there is only one quantum of conductance associated with the electromagnetic environment, regardless of the number of separate electrical connections.

We introduce a device representative of structures used for measurements of thermal properties as well as for bolometric detectors. In Fig. 1(a), a submicron scale normal-metal thin-film element is placed on a nanofabricated suspended dielectric paddle. Superconducting leads provide electrical contact, and effectively eliminate the thermal conductivity due to electron diffusion [10]. The metal film is represented as a lumped resistive element, connected to the electromagnetic environment through a transmission line, in Fig. 1(b). We distinguish the electrical environment, comprising the transmission line and electrical circuit connected to it, from the radiative environment, to which the electron gas is coupled only via free-space (blackbody) radiation. Our current understanding of the thermal relaxation of this system is the result of an active theoretical and experimental effort, summarized in Fig. 1(c). Over short time scales, electrons in a diffusive metal equilibrate with one another through electron-electron scattering (see, e.g., [11] and references therein). The electron gas, at temperature T_e, then equilibrates over longer times with the local phonon environment at $T_{\rm ph}$ via electron-phonon interactions [9,12–16]. The thermal link between the electrons and phonons becomes very weak at low temperatures [12,13]. For a metal with volume V, the power flow $P_{e\text{-ph}}$ from the electrons to the phonons is

$$P_{e\text{-ph}} = \Sigma V (T_e^n - T_{\rm ph}^n), \tag{1}$$

where the power $n \cong 5$ depends upon details of the Fermi surface and phonon dispersion, and Σ is a material-dependent parameter [17]. For small temperature differences $|T_e - T_{\rm ph}| \ll T_{\rm ph}$, the effective electron-phonon thermal conductance is $G_{e\text{-ph}} \equiv dP_{e\text{-ph}}/dT = 5\Sigma V T^4$.

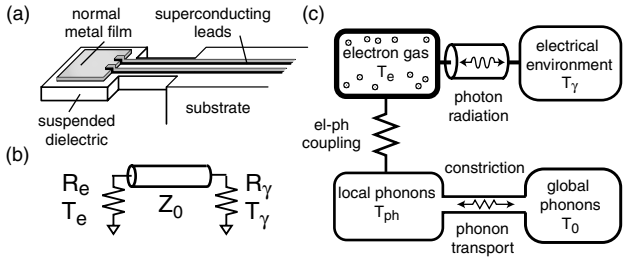

FIG. 1. (a) Representative device: a normal metal film on a suspended dielectric structure, connected with superconducting leads. (b) Electrical schematic: The normal metal film is shown as a resistor, R_e, connected to the electromagnetic environment with impedance Z_γ, via a transmission line with impedance Z_0. (c) Parallel thermal pathways: Diffusive electron gas at temperature T_e equilibrates through electron-phonon coupling with the local phonons at $T_{\rm ph}$, which in turn equilibrate with the global phonons at T_0 through a mechanical constriction. The electrons are also coupled to the electromagnetic environment at temperature T_γ via photon radiation.

Interest in the thermal physics of nanostructures can be traced back to investigations of the fundamental bounds on information processing and transfer [18,19]. In this context, Pendry [2] calculated that the thermal conductance associated with single mode, phase-coherent transport of degenerate fermions and of massless bosons is $G_Q \equiv \pi^2 k_B^2 T/3h$, where $G_Q \approx 1$ pW/K at 1 K. For electrons in a degenerate Fermi gas, the thermal conductivity is $G_e = \mathcal{T} N G_Q$ for N channels each with transmission coefficient $\mathcal{T}$ [3,4]. The phonon thermal conductance through a doubly clamped beam, such as in Fig. 1(a), occurs via four independent transmission modes at low T, each with transmission $\mathcal{T}$; therefore $G_{\rm ph} = 4\mathcal{T} G_Q$ [5–9].

The present understanding of the thermal relaxation is that the electrons in the metal equilibrate with the phonons in the dielectric paddle, which then equilibrate with the bulk through the quantized phonon conductance. There is, however, a significant *photon* contribution to this equilibration, in parallel with that due to phonons, and at low temperatures the photonic contribution dominates. This is due to transport of thermal photons through the electrical leads [20–22], and dominates when the object is smaller than the thermal photon wavelength [2]. Present experimental efforts are already in the size and temperature range for which this contribution can dominate, with implications for measurements of thermal relaxation, and applications in calorimetry and bolometry.

Below $T = 1$ K, thermal photons have frequencies $\nu_{\rm th} \equiv k_B T/h$, with wavelengths $\lambda_{\rm th} = c/\nu_{\rm th} > 1$ cm. A diffusive electron gas, with dimensions less than 1 mm $\ll \lambda_{\rm th}$, can be represented by an electrical impedance $Z_e(\nu)$. In thermal equilibrium, the electron temperature T_e is directly related to the noise emitted by this impedance. In practice, the electron gas is connected via measurement leads to an electrical circuit, which presents an environmental impedance $Z_\gamma(\nu)$ to the electron gas. The noise associated with this impedance is, in many cases, represented by a temperature T_γ, with $T_\gamma \approx T_0$ the cryostat temperature. The electron and environmental noise sources cause the exchange of energy between the two systems, and is an example of one-dimensional blackbody radiation [21,22]; for an electron gas with a sufficiently small surface area, this dominates over the free-space radiation described by the Stefan-Boltzmann T^4 law.

In the simplest situation, the electron and environmental impedances Z_e and Z_γ may be represented by two resistors, R_e and R_γ, with noise temperatures T_e and T_γ. The electromagnetic noise power radiated from these resistors is quantified by the fluctuation-dissipation theorem [23]. The voltage noise density for a resistance R at temperature T is $S_V(\nu) = 2h\nu R \coth(\nu/2\nu_{\rm th})$, where $\nu \geq 0$. At low frequencies $\nu \ll \nu_{\rm th}$, this is the usual Nyquist result $S_V = 4k_B TR$, while for high frequencies $S_V \to 2h\nu R$, the "quantum noise" limit. We can easily rewrite the voltage noise density in terms of the Bose-Einstein distribution $n(\epsilon) = [\exp(\epsilon/k_B T) - 1]^{-1}$ of the photons emitted by the resistor,

$$S_V(\nu) = 4h\nu R[\, n(h\nu) + \tfrac{1}{2}\,]. \tag{2}$$

The electrons, with $R = R_e$, emit this voltage noise, generating a current noise through both the electron and the environmental impedances, $S_I = S_V/(R_e + R_\gamma)^2$, so that the noise power $S_e = R_\gamma S_I$ absorbed by the environment, ignoring the zero-point term, is

$$S_e(\nu) = \frac{R_\gamma}{(R_e + R_\gamma)^2} 4h\nu R_e n_e(h\nu), \tag{3}$$

where $n_e(h\nu)$ evaluated at $T = T_e$. There is a similar expression for the noise power S_γ emitted by the environment and absorbed by the electrons, with the subscripts e and γ exchanged in (3).

The net electromagnetic (photon) power flowing from the electrons to the environment is given by

$$\begin{aligned} P_\gamma &= \int_0^\infty [S_e(\nu) - S_\gamma(\nu)]\, d\nu \\ &= r \int_0^\infty h\nu [n_e(h\nu) - n_\gamma(h\nu)]\, d\nu, \end{aligned} \tag{4}$$

where we define the coupling coefficient $r = 4R_e R_\gamma/(R_e + R_\gamma)^2$. This coupling coefficient is closely related to the transmission coefficient $\mathcal{T}$ appearing in the formulas for G_e and G_p, the thermal conductance of electrons and phonons. Here the transmission line is assumed to have unit transmissivity, but the coupling to and from the transmission line is embedded in the coefficient r; in the case of the electron and phonon single-channel formulas, the coefficient $\mathcal{T}$ includes both the coupling *and* the transmissivity of a channel. The power flow is positive if T_e is greater than T_γ. In Fig. 2, we show the spectral power densities S_e, S_γ, and their difference, in dimensionless units $S/rh\nu_{\rm th}$, as a function of dimensionless frequency $\nu/\nu_{\rm th} = k_B T_\gamma \nu/h$. The net noise

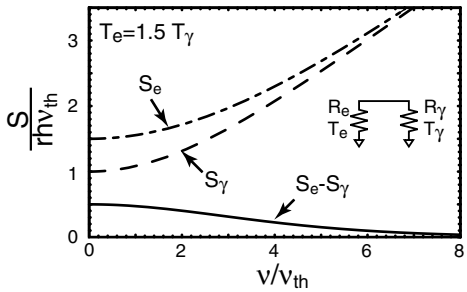

FIG. 2. Noise power densities S_e, S_γ, and their difference, plotted as a function of dimensionless frequency $\nu/\nu_{\rm th}$, for $T_e = 1.5T_\gamma$, and $\nu_{\rm th}$ evaluated at T_γ. The inset shows equivalent circuit.

power extends from $\nu = 0$ to $\nu \sim 5\nu_{\rm th}$, a frequency range of about 10 GHz at $T = 100$ mK.

The power flow can be characterized by an effective photon thermal conductance $G_\gamma = dP_\gamma/dT$, with

$$G_\gamma = r\int_0^\infty h\nu \frac{d}{dT}\frac{1}{\exp(h\nu/k_BT)-1}d\nu = rG_Q. \quad (5)$$

For matched resistances $R_e = R_\gamma$, the coupling coefficient $r = 1$, and the thermal conductance G_γ is equal to the quantum of thermal conductance G_Q. Mismatched resistances reduce the thermal conductance from this value by the temperature-independent scale factor $r < 1$.

The thermal conductance G_γ associated with the electromagnetic coupling is therefore proportional to the quantum of thermal conductance. Any measurement of the total thermal conductance G of an electron gas to its environment will include this contribution. In the absence of direct electron transport-mediated pathways, the other primary thermal path is due to electron-phonon coupling $G_{e\text{-ph}}$, with subsequent phonon transport to the global phonon environment $G_{\rm ph}$, yielding an effective phonon-mediated conductance $(1/G_{e\text{-ph}} + 1/G_{\rm ph})^{-1}$. At very low temperatures, the electron-phonon coupling becomes very weak, scaling as T^4, and will become negligible in comparison with the photonic contribution: The total electron thermal conductance G therefore approaches G_γ as $T \to 0$. For matched resistances $R_e = R_\gamma$, the crossover occurs at the temperature $T_{\rm cr} \equiv (\pi^2 k_B^2/15h\Sigma V)^{1/3} \simeq 50\ {\rm mK}/(V/\mu{\rm m}^3)^{1/3}$. Typical nanoscale electron volumes of 0.001–0.1 μm^3 thus yield crossover temperatures of 500–100 mK: This is clearly a significant correction for small electron volumes at temperatures easily reached with ^{3}He cryostats, ^{3}He:^{4}He dilution refrigerators, or adiabatic demagnetization refrigerators.

Figure 3 shows the temperature dependence of the total thermal conductance G from an electron gas to its environment, including both photon and phonon contributions. We set $R_e = R_\gamma$, so $G_\gamma = G_Q$, and use the phonon conductance due to a single insulating beam, with $G_{\rm ph} = 4G_Q$. At very low temperatures, $G_e \to G_Q$, due to photon conductance. At higher temperatures, $G \to 5G_Q$, due to the sum of contributions from phonon- and photon-mediated transport. More generally, the transition from single-mode conductance to the higher temperature limit of $N + 1$ conducting phonon modes occurs over the range from $T_{\rm cr}$ to $(N+1)^{1/3}T_{\rm cr}$.

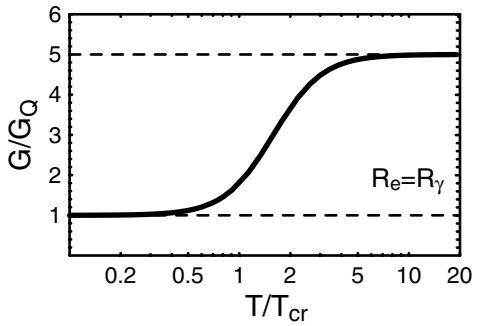

FIG. 3. Thermal conductance G/G_Q as a function of $T/T_{\rm cr}$ for an electron gas relaxing via phonons and photons. The solid line is the total thermal conductance; the dashed lines are the high T limit of parallel phonon- and photon-mediated conductance, and the low T limit of purely photon-mediated conductance.

Measurements of thermal conductance at low temperatures in nanostructures must take this photon-mediated cooling into account. Such measurements can make significant errors in two ways: The thermal power P can be significantly different from the power P_e applied by the experimenter to the electron gas, and the thermometer can report a temperature substantially different from the actual temperature. These corrections should be included in analyses of electron and phonon thermal conductances; in those to date [7,9,14,15], the electron volumes were sufficiently large, and the electron resistances sufficiently mismatched to the environmental impedance, so this correction is likely to be small.

We have assumed that the electrical connection between the electron gas and environmental resistances R_e and R_γ could be treated as frequency independent and lossless. The electromagnetic environment will more generally present a complex impedance $Z_\gamma(\nu)$, changing the associated thermal conductance in (5) to

$$G_\gamma = \frac{k_B^2 T}{h}\int_0^\infty \tilde{r}(x\nu_{\rm th})\frac{x^2 e^x}{(e^x-1)^2}dx, \quad (6)$$

with the coupling coefficient $\tilde{r}(\nu)$ given by $\tilde{r}(\nu) = 4R_e\,{\rm Re}[Z_\gamma(\nu)]/|R_e + Z_\gamma(\nu)|^2$, and $x = \nu/\nu_{\rm th}$. This allows the environment to include reactive as well as dissipative elements. Here we extend our model calculation to one particular impedance model, one in which the physical separation L between the two resistors R_e and R_γ is nonzero. If L is of the order of, or longer than, the characteristic thermal wavelength $\lambda_{\rm th} = c_\phi/\nu_{\rm th} = hc_\phi/k_BT$, for a transmitting network with signal velocity c_ϕ, the finite signal velocity must be included. For an environment at $T_\gamma = 100$ mK, this would be appropriate for resistors separated by a distance larger than about $L \simeq 1$ cm. We include this by modeling the leads as a lossless transmission line terminated by R_γ, with characteristic impedance Z_0 and electrical delay $\Delta t = L/c_\phi$. This changes the effective environmental impedance to

$$Z_\gamma(\nu) = \frac{R_\gamma + iZ_0\tan(2\pi\nu\Delta t)}{Z_0 + iR_\gamma\tan(2\pi\nu\Delta t)}Z_0. \quad (7)$$

The form of the integrand in (6) then depends strongly on the relation between R_γ and the transmission line impedance Z_0: For $R_\gamma = Z_0$ (the case for a properly terminated transmission line), then $Z_\gamma(\nu) = R_\gamma$ and the integrand in

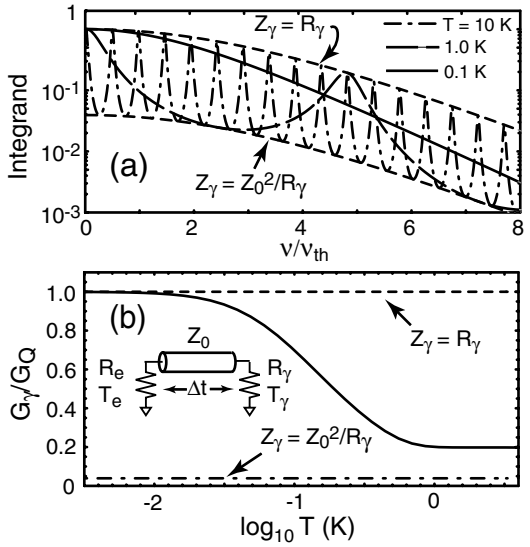

FIG. 4. (a) Integrand from (6) as a function of frequency $\nu/\nu_{\rm th}$, plotted for different T. Also shown are the limits of the integrand, for maximum and minimum values $Z_\gamma = Z_0^2/R_e$ and R_e. (b) Calculated thermal conductance G/G_Q as a function of T, showing transition from unity at low T to the limit $Z_\gamma = Z_0^2/R_\gamma = 1\ \mathrm{k}\Omega$.

(6) is independent of frequency, yielding the same result as in (5). For $R_\gamma \neq Z_0$, the effective impedance $Z_\gamma(\nu)$ varies periodically in frequency between the limiting values R_γ and Z_0^2/R_γ, with a period $\Delta\nu = c_\phi/2L = 1/2\Delta t$. The integral in (6) smoothes out these oscillations.

In Fig. 4(a), we display the integrand in (6), for a model thermometer and environment in which the two resistors are equal, $R_e = R_\gamma = 10\ \Omega$, and are connected by an ideal transmission line with $Z_0 = 100\ \Omega$ and a delay $\Delta t = 5$ ps. These values are realistic ones for an actual experimental implementation. The oscillations in frequency apparent in Fig. 4(a) become more rapid as the temperature increases, and are bound on either side by the low and high impedance limits of $Z_\gamma = R_\gamma$ and $Z_\gamma = Z_0^2/R_\gamma$. In Fig. 4(b), we show the resulting thermal conductance G_γ for the same model, which at the lowest temperatures reaches the value G_Q, as then $Z_\gamma(\nu) = R_\gamma$ for the relevant frequencies, yielding $\tilde{r} = 1$. At higher temperatures, the conductance approaches the limit $r'G_Q$ with the smaller resistance factor $r' = 4R_e(Z_0^2/R_\gamma)/(R_e + Z_0^2/R_\gamma)^2 \simeq 0.04$. It does not quite reach this value because the oscillations give a frequency-averaged resistance ratio above this lower limit.

In conclusion, we have shown that the thermal conductance G_γ due to electromagnetic coupling provides a very important relaxation process for a nanoscale electron system at low temperatures. Power deposited in the electron gas can be reradiated as low frequency photons rather than phonons. This additional pathway for thermal relaxation can have important implications for the design of low-temperature bolometers, significantly affecting their response time and sensitivity.

We thank Konrad Lehnert for valuable conversations. We acknowledge financial support provided by the NASA Office of Space Science under Grants No. NAG5-11426 (D. R. S. and A. N. C.) and No. NAG5-11425 (R. J. S.).

*Electronic address: cleland@physics.ucsb.edu

[1] B. J. van Wees, H. van Houten, C. W. J. Beenakker, J. J. G. Williamson, L. P. Kouwenhoven, D. van der Marek, and C. T. Foxon, Phys. Rev. Lett. **60**, 848 (1988).
[2] J. B. Pendry, J. Phys. A **16**, 2161 (1983).
[3] L. W. Molenkamp, T. Gravier, H. van Houten, O. J. A. Buijk, M. A. A. Mabesoone, and C. T. Foxon, Phys. Rev. Lett. **68**, 3765 (1992).
[4] A. Greiner, L. Reggiani, T. Kuhn, and L. Varani, Phys. Rev. Lett. **78**, 1114 (1997).
[5] L. G. C. Rego and G. Kirczenow, Phys. Rev. Lett. **81**, 232 (1998).
[6] M. P. Blencowe, Phys. Rev. B **59**, 4992 (1999).
[7] K. Schwab, E. A. Henriksen, J. M. Worlock, and M. L. Roukes, Nature (London) **404**, 974 (2000).
[8] K. Patton and M. Geller, Phys. Rev. B **64**, 155320 (2001).
[9] C. S. Yung, D. R. Schmidt, and A. N. Cleland, Appl. Phys. Lett. **81**, 31 (2002).
[10] Thermal isolation may also be achieved through other means including resistive or capacitively coupled electrical leads.
[11] H. Pothier, S. Guéron, N. O. Birge, D. Esteve, and M. H. Devoret, Phys. Rev. Lett. **79**, 3490 (1997).
[12] W. A. Little, Can. J. Phys. **37**, 334 (1959).
[13] V. F. Gantmakher, Rep. Prog. Phys. **37**, 317 (1974).
[14] M. L. Roukes, M. R. Freeman, R. S. Germain, R. C. Richardson, and M. B. Ketchen, Phys. Rev. Lett. **55**, 422 (1985).
[15] F. C. Wellstood, C. Urbina, and J. Clarke, Phys. Rev. B **49**, 5942 (1994).
[16] E. Chow, H. P. Wei, S. M. Girvin, and M. Shayegan, Phys. Rev. Lett. **77**, 1143 (1996).
[17] For Cu, $\Sigma \simeq 2 \times 10^9\ \mathrm{W/m^3\,K^5}$ [9,14,15]. In a larger collection of material systems, n has been found to be in the range 4–6. See, e.g., [16].
[18] J. D. Bekenstein, Phys. Rev. Lett. **46**, 623 (1981).
[19] D. Deutsch, Phys. Rev. Lett. **48**, 286 (1982).
[20] H. Nyquist, Phys. Rev. **32**, 110 (1928).
[21] R. Dicke, Rev. Sci. Instrum. **17**, 268 (1946).
[22] F. Reif, *Fundamentals of Statistical and Thermal Physics* (McGraw-Hill, New York, 1965).
[23] H. B. Callen and T. A. Welton, Phys. Rev. **83**, 34 (1951).